

# Experimental identification of rare-earth magnetic suspensions for micro and meso scale levitating systems

Chamila Siyambalapitiya<sup>1</sup>, Giorgio De Pasquale\*<sup>2</sup> and Aurelio Somà<sup>2</sup>

<sup>1</sup>*Electrical Engineering Department, University of South Florida, 4202 East Fowler Avenue, 33620, Tampa, USA*

<sup>2</sup>*Department of Mechanics and Aerospace Engineering, Politecnico di Torino, Corso Duca degli Abruzzi 24, 10129 Torino, Italy*

*(Received May 27, 2011, Revised April 28, 2012, Accepted June 28, 2012)*

**Abstract.** Magnetic suspensions based on passive levitation of diamagnetic materials on permanent magnets provide attractive systems for several applications on the micro and meso scales. The magnetic properties of these kinds of suspensions dramatically reduce the global mechanical stiffness of the devices providing significant effects on their dynamic response. The goal of this paper is to investigate the static and dynamic behavior of magnetic suspensions with respect to its dependant parameters. Experimental measurements have been performed on the response of dedicated prototypes where the geometrical dimensions and magnetic field strength have been intended as variable parameters. Some benefits have been documented in the fields of energy harvesting and inertial sensing, while additional applications of magnetic suspensions are under investigation.

**Keywords:** magnetic levitation; diamagnetism; NdFeB; pyrolytic graphite; dynamic response

---

## 1. Introduction

The magnetic levitation principle includes the following categories: active levitation with electromagnets, and passive levitation with permanent magnets and superconductors. Active levitation has the advantage of the user controllability (e.g., levitating bearings, Maglev trains, etc.); however it consumes massive power and requires expensive and complex feedback systems. Passive permanent magnet levitation has been investigated by several groups and is based on the repulsive force generated between two permanent magnets facing opposing polarity to levitate a third magnet facing the same polarity. This method is highly unstable and is limited to a few applicable materials. Passive diamagnetic levitation is produced by the magnetic force acting on a diamagnetic material when an external magnetic field is present. The benefits of a passive diamagnetic levitation system using permanent magnets lie in minuscule power consumption, the room temperature applicability and self-stabilization over its state of the art counterparts.

Diamagnetic materials can induce a magnetic field within themselves in opposition to an outer magnetic field, producing a repulsive force; these materials are identified by negative magnetic susceptibility values. The lowest magnetic susceptibility value of -1 belongs to superconductors.

---

\*Corresponding author, Dr., E-mail: [giorgio.depasquale@polito.it](mailto:giorgio.depasquale@polito.it)

While the invention of active levitation of objects dates back to the 1940's, the passive levitation of diamagnetic materials using permanent magnets has been shown in recent years following the discovery of NdFeB magnets in the mid 90's (Pelrine 1995).

Magnetism related MEMS devices have not been intensively exploited to the extent of electrical devices mainly due to the limits in manufacturing processes. The availability of the strongest permanent magnets (NdFeB) opened up venues to use passive levitation on devices for several different applications such as micro and meso inertial sensing devices, power generation, energy harvesting, etc. (Garmire *et al.* 2007, Yeatman 2007). Micro-systems such as micro-manipulators for high-precision positioning, bearings, resonators, contact-free micro-handlers, and contamination free lab-on-chip devices can be strongly improved by implementing the diamagnetic levitation concept.

The small size of characterizing proof-masses in micro-devices usually results in high natural resonance frequencies of the system to a level that is not applicable within the energy harvesting from environmental vibrations which are typically a few orders of magnitude lower than the resonance frequency range of the micro-device. The diamagnetic levitation is a promising field of technology that opens up a new generation of suspensions in both micro and macro systems, in which traditional stiffer mechanical suspensions are replaced by low stiffness magnetic suspension (Tang *et al.* 1992, Chyuan and Liao 2005, Krishnamoorthy *et al.* 2008, Mann and Sims 2009). Furthermore, in the case of energy harvesters, the nature of magnetic suspensions does not reduce the efficiency of the generator. The application of levitating suspensions to energy harvesters is particularly promising for capacitive and inductive generators. In capacitive generators, the diamagnetic levitated proof mass is used as the movable armature of a variable capacitor that modifies its charge or voltage when subjected to vibrations. Additionally the comb-drive electrodes layout can be used to increase the active surface of the capacitor. The power generation can be improved by depositing layer of electret material on the variable capacitive arm. In inductive harvesters, the levitation of a permanent magnet under a magnetic force induced by another magnet with the same polarity is the preferred strategy; in this case, the levitating magnet oscillates in a solenoid under the effect of vibrations producing the electric current flow. In both cases, the magnetic suspension provides low stiffness and tunability to the harvesters.

Other advantages of levitating suspensions are given by the removal of mechanical bending elements, which are often the source of energy dissipation through thermo-elastic damping and air damping under the suspensions. Element bending also affects the device reliability and durability due to mechanical fatigue. An additional benefit deriving from the magnetic levitation is the prevention of stiction effects between the proof-mass and the substrate. This problem is very common in micro scale devices, particularly those related to biology which operates in liquid or humid environments. Obstacles associated with stiction can be avoided by the diamagnetic levitation approach, as the force between the device and the substrate is repulsive thus preventing contact.

Some theoretical studies related to modeling of magnetic suspensions on the micro and macro scale have been conducted (Chetouani *et al.* 2007, Barrot 2008) in which the magneto-structural coupling was considered. Also, it was shown (Elbuken *et al.* 2006) that eddy currents may be used to increase the damping of the levitating mass and to reduce undesired vibrations. However, experimental measurements of static and dynamic behavior of magnetic suspensions are not very widespread in the literature (Garmire *et al.* 2007, De Pasquale *et al.* 2009, De Pasquale *et al.* 2010).

In this study, the static behavior and the dynamic response of magnetic suspensions and dependent parameters are investigated; a few relations useful for the designer are also introduced. The experimental results of the effects of the magnetic field strength and diamagnetic proof-mass geometry on the

levitation height and dynamic response are documented. Similar parametric characterizations have been previously reported (Alqadi *et al.* 2007) in the analytic formulation. The prototype of the suspension considered is in the meso-scale due to ease of fabrication and assembly; the microfabrication techniques for building micro permanent magnets are not well established at present, even if some promising samples are leaving the laboratories (Chetouani *et al.* 2007, Kauffmann *et al.* 2010).

## 2. The suspension prototype

The magnetic suspension prototype is composed of four square permanent magnets, oriented in the ‘opposite’ configuration (Barrot 2008) and forming a planar layer as shown in Fig. 1. The number of magnet layers ( $N$ ) is varied to increase the intensity of the magnetic field during the characterization. The permanent magnets are made of NdFeB alloy and the surface has been metallic coated with Ni-Cu-Ni. Square, pyrolytic graphite diamagnetic proof-masses with varied dimensions are used as the levitating component of the suspension. The dimensions of magnets and graphite proof-masses are reported in Table 1.

## 3. Modeling

The equilibrium condition of the proof-mass is the result of the opposing effects of the gravitational force ( $F_g$ ) and the magnetic force ( $F_m$ ). The magnetic force is generated by a secondary magnetic field that is induced inside the diamagnetic material when an external magnetic field is present. The orientation of this force allows the repulsive effect between the proof-mass and

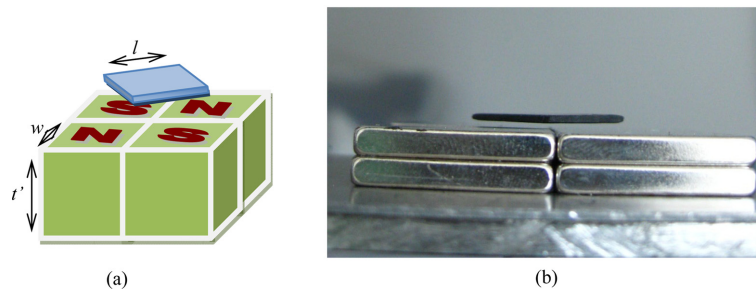


Fig. 1 (a) Schematic of the magnetic suspension prototype with parameterized geometry and (b) lateral image of the levitating system

Table 1 Magnetic suspension properties

Description	Symbol	Value	Unit
NdFeB magnets side	$W$	20	mm
NdFeB magnets thickness	$t'$	3	mm
NdFeB magnets layers	$N$	1-2-3	-
pyrolytic graphite side	$L$	9-10-11-12-13-14	mm
pyrolytic graphite thickness	$T$	0.3-0.5-0.7-0.9-1-1.1	mm
pyrolytic graphite density	$\rho$	2200	kg/m <sup>3</sup>

the permanent magnets, hence the levitation.

The magnetic force per unit volume ( $f_m=F_m/V$ ) acting on the levitating proof-mass can be calculated as

$$f_m \approx \frac{1}{2\mu_0} \chi_m \cdot \text{grad}(\vec{B}^2) \quad (1)$$

and the overall magnetic force as

$$F_m \approx \int \frac{1}{2\mu_0} \chi_m \cdot \text{grad}(\vec{B}^2) dV \quad (2)$$

with magnetic permeability ( $\mu_0$ ), magnetic susceptibility ( $\chi_m$ ), and magnetic flux density ( $\vec{B}$ ). By considering that the magnetic force equals the gravity force in each equilibrium position, i.e.,  $F_m=F_g=\rho Vg$ , with density ( $\rho$ ), volume ( $V$ ), and gravitational acceleration ( $g$ ), results in

$$\int \frac{1}{2\mu_0} \chi_m \cdot \text{grad}(\vec{B}^2) dV = \rho Vg \quad (3)$$

when the proof-mass is in a static equilibrium levitating state. The distribution of the magnetic field can be calculated by analytic formulations present in the literature that are able to estimate the value of  $\vec{B}$  in the region surrounding the magnets (Barrot 2008).

Fig. 2 represents the single degree of freedom (*dof*) model of the levitating suspension, where the mass ( $m$ ) of the levitating diamagnetic material, the magnetic stiffness ( $k_m$ ) given by the repulsive effect, the viscous damping ( $c_v$ ) due to the compression of air when the plate is moving, and the magnetic damping ( $c_m$ ) due to the parasitic currents in the diamagnetic material. The effect of parasitic currents is often negligible if the proof-mass is composed of graphite; this parameter becomes relevant in the presence of the metal coating of the diamagnetic material.

By neglecting the damping sources, and assuming a driving force with the form  $F(t)=f_0 \cdot \sin(\omega t)$ , the simplified relation is given by

$$k_m = \omega^2 m \quad (4)$$

where  $\omega$  is the angular frequency, which estimates the magnetic stiffness in the case of small oscillations. In static conditions,  $k_m$  is proportional to the ratio  $F_m(z)/z$ ; the magnetic stiffness is nonlinear with respect to the vertical position  $z$ , as the magnetic flux density  $\vec{B}$  nonlinearly depends on  $z$ . The nonlinear equations describing the behavior of the system for large displacements are generally too complicated to be solved with close-form solutions; in this case, numerical methods based on direct integration can provide the solution of the motion equations.

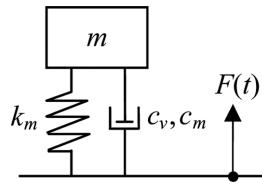


Fig. 2 Single dof model of the levitating magnetic suspension

## 4. Experimental identification

### 4.1 Magnetic field measurement

The distribution of the magnetic field generated by the permanent magnets was measured by means of a magnetometer (AlphaLab DC). The dimensions of the magnetometer sensing tip were  $0.2 \times 0.2$  mm. A computerized 3-axial stage (Newport M-460A) was used to move the magnets and to provide position control. The stage was moved by discrete steps (1 mm in horizontal directions, 0.2 mm in vertical direction) providing a map of the field distribution. The measurement set-up is represented in Fig. 3.

### 4.2 Levitation height detection

The levitation height of the diamagnetic proof-mass above the magnets was measured by an

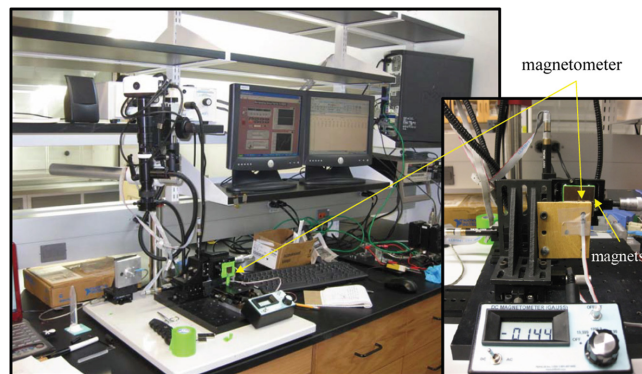


Fig. 3 Experimental set-up for the magnetic flux measurement

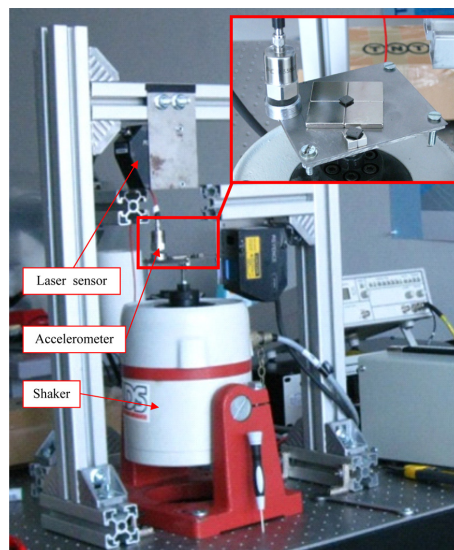


Fig. 4 Experimental set-up for the dynamic behavior characterization

optical laser sensor (Keyence LK-G82), with 50 kHz maximum sampling frequency and  $0.2 \mu\text{m}$  0.05% accuracy. This optical technique was used to evaluate the proof-mass position in both static (equilibrium state) and dynamic (time-dependent displacement due to base excitation) conditions. The dynamic tests were performed by applying a driving force to the suspension by means of an electro-mechanical shaker (Tira TV51120), which simulates environmental vibrations. The shaker was driven by a sinusoidal function generator and a power amplifier; the closed-loop feedback signal of the excitation system was provided by an acceleration sensor. The complete testing set-up for dynamic tests is represented in Fig. 4.

## 5. Results

### 5.1 Magnetic field distribution

The measured values of the magnetic flux density are reported in Fig. 5. The magnetic flux density values for the space region above the magnets were measured with the aid of the magnetometer to map the flux distribution. The volume represented in the inset illustrates the measurement region. The surfaces reported in the diagram refer to the corresponding distance ( $z$ )

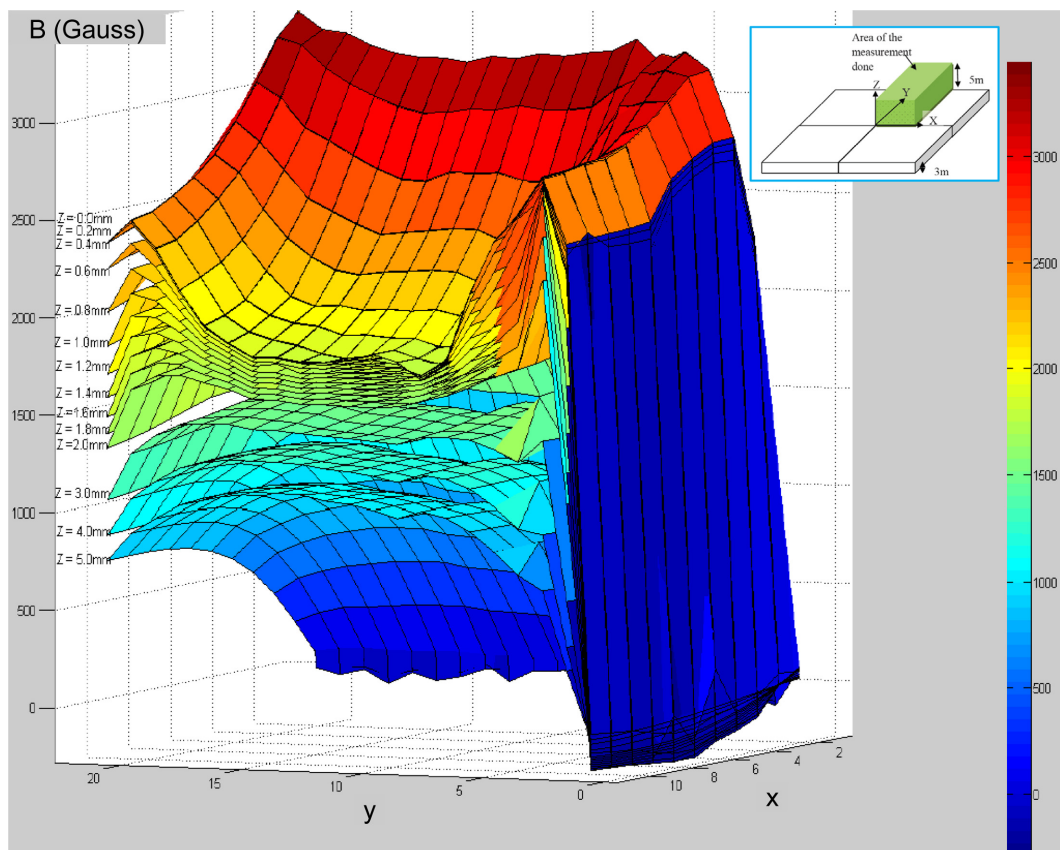


Fig. 5 Measured flux density for different  $z$  values above the permanent magnet surface

from the magnets surface, indicated on the left of the figure. A quadrant of the measured magnetic flux is shown for simplicity, while illustrating the non-uniform flux distribution. At the interfaces of the magnets the flux is zero; it quickly increases within 1-2 mm of the interface, then gradually decreases and plateaus over the center region of each magnet. Note that the highest magnetic flux occurs closest to the magnet surface and decreases while becoming more uniform as the  $z$  height increases. These effects are a result of the field superimposition of the opposing neighboring magnets and are repeated in the region over each magnet. The authors reported the FEM simulation of the magnetic field distribution in (De Pasquale *et al.* 2012), where the estimation of the magnetic force acting on the diamagnetic proof mass is also presented.

### 5.1 Static behavior

The static behavior of the suspension was investigated for several different dimensions of proof-masses, considering area and thickness as variable parameters. The configuration of the oriented NdFeB permanent magnets (Fig. 1) is obtained by four square pieces (side  $w = 20$  mm, thickness  $t' = 3$  mm); the number of layers of magnets is changed ( $1 \leq N \leq 3$ ) to vary the magnetic field (Table 1). The static levitation height of the proof-masses with varied thicknesses (side  $l = 10$  mm) were measured by the laser displacement sensor by focusing on the center of the proof-mass; the relation between the graphite thickness ( $t$ ) and the levitation height from the top of the magnets to the center-of-mass of the proof-mass is shown in Fig. 6. A similar characterization was performed for fixed thickness ( $t = 1$  mm) by varying the graphite area, results are reported in Fig. 7.

### 5.2 Dynamic behavior

The dynamic response of the suspension was obtained for different dimensions of its components. The force transferred by the shaker was adjusted to provide a constant acceleration to the suspension base and to provide consistent comparison throughout the measurements. The driving frequency was swept from 0 - 20 Hz. The oscillation amplitude of the excitation was kept to a small scale ( $< 0.5$  mm) to avoid irregular motions of the proof-mass. It was observed that the motion of

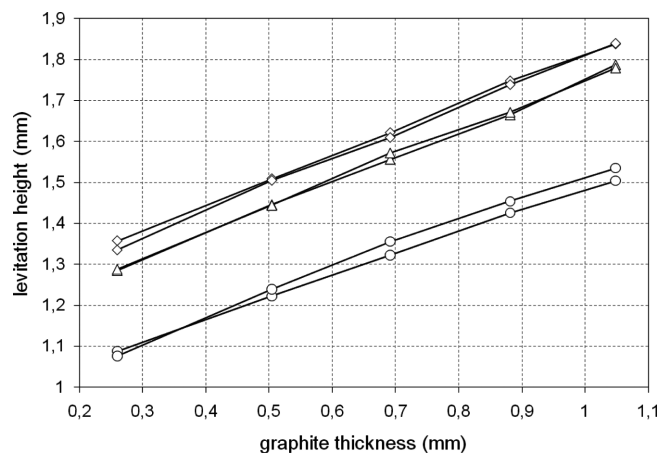


Fig. 6 Levitation height of graphite with variable thicknesses ( $t$ ) in presence of one (○), two (△) and three (◇) layers of NdFeB permanent magnets; two samples have been tested for each configuration

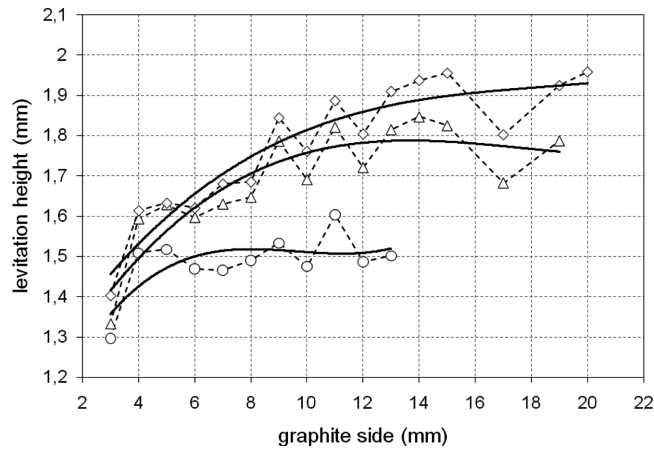


Fig. 7 Levitation height of graphite with variable side lengths ( $l$ ) in presence of one ( $\circ$ ), two ( $\triangle$ ) and three ( $\diamond$ ) layers of NdFeB permanent magnets

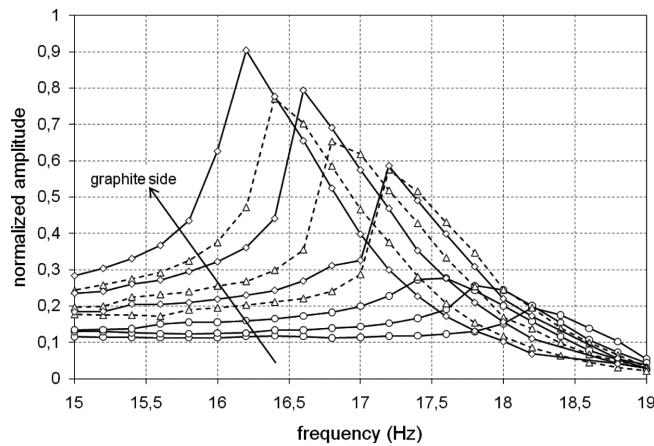


Fig. 8 Dynamic response of the suspension for graphite side lengths ( $l$ ) of 9, 10 and 11 mm in the presence of one ( $\circ$ ), two ( $\triangle$ ) or three ( $\diamond$ ) layers of NdFeB permanent magnets

the graphite proof-mass became more stable with larger graphite proof-masses. The dynamic behavior results are shown in Fig. 8 for increasing graphite side length ( $l = 9, 10, 11$  mm) and number of layers of NdFeB magnets ( $N = 1, 2, 3$ ). The dynamic response curves were then used to determine the resonance frequency of the system and to calculate its equivalent stiffness.

## 6. Discussions

### 6.1 Static and dynamic behavior

The graphs reported in Fig. 6 reveal a linear relation between the graphite thickness ( $t$ ) and the levitation height, within the range considered. This proportionality testifies that the contribution of additional diamagnetic material (volume is proportional to thickness) produces a variation of the

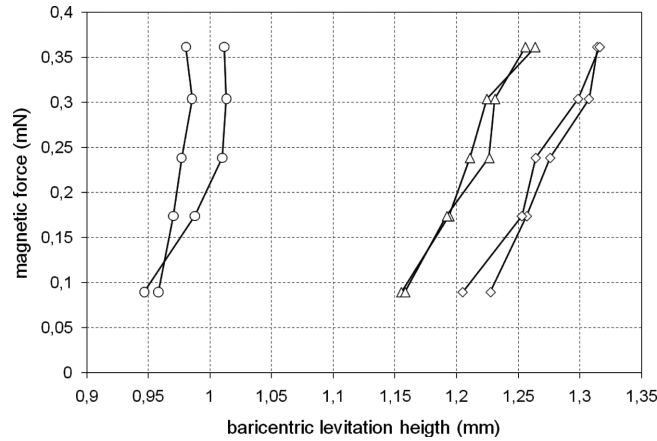


Fig. 9 Magnetic force ( $F_m$ ) calculated from the static equilibrium of proof-masses with different thicknesses ( $t$ ) in presence of one (○), two (△) and three (◇) layers of NdFeB permanent magnets

magnetic force that is larger than the increments of the gravity force acting on the proof-mass. The ratio between the variations of magnetic and gravity forces ( $\Delta F_m > \Delta F_g$ ) causes the center-of-mass of the proof-mass to levitate at higher heights. This effect can be explained by considering that the magnetic field generated inside the diamagnetic graphite is opposite in direction to the field generated by permanent magnets; the entity of this induced field is proportional to the volume of the proof-mass. The same effect is exhibited by increasing the graphite area (Fig. 7); however in this case, after the first region ( $l < 8$  mm), the gravity force increment due to additional mass equals the increment of magnetic force, i.e.,  $\Delta F_m \approx \Delta F_g$  for  $l > 8 - 9$  mm.

Starting from the static measurements of the levitating position, it is possible to calculate the magnetic force ( $F_m$ ) acting on the diamagnetic proof-mass in equilibrium conditions by using Eq. (3); the results are reported in Fig. 9.

The dynamic characterization performed was limited to small oscillations of the mass, since the overall magnetic stiffness ( $k_m$ ) is linear in the  $z$  direction around the levitating position. As a

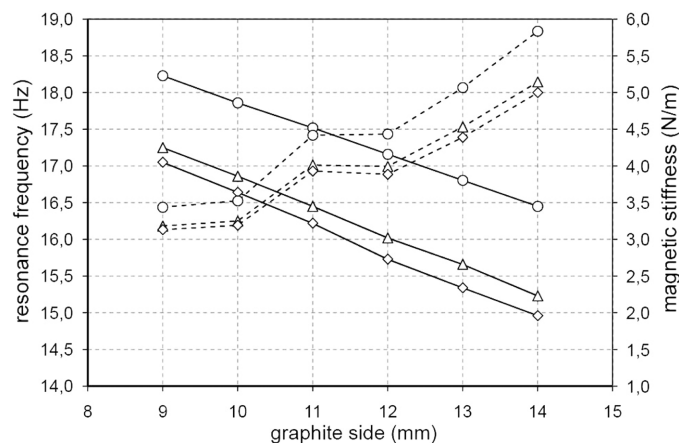


Fig. 10 Resonance frequency (continuous) and dynamic magnetic stiffness (dashed) of the suspension in presence of (○), two (△) and three (◇) layers of NdFeB permanent magnets

Table 2 Experimental results of resonance frequency and magnetic stiffness ( $k_m$ ) for one, two and three layers of magnets

Graphite side $w$ (mm)	Resonance frequency $f$ (Hz)			Magnetic stiffness $k_m$ (N/m)		
	$N=1$	$N=2$	$N=3$	$N=1$	$N=2$	$N=3$
9	18.2	17.2	17.0	2.44	2.18	2.13
10	17.9	16.9	16.6	2.53	2.25	2.19
11	17.5	16.4	16.2	3.42	3.01	2.93
12	17.2	16.0	15.7	3.43	2.99	2.89
13	16.8	15.7	15.3	4.07	3.53	3.39
14	16.4	15.2	15.0	4.84	4.15	4.00

consequence, Eq. (4) can be used to estimate  $k_m$  in this small interval. Fig. 10 and Table 2 report the variation of resonance frequency and stiffness of the suspension when the graphite area is increased; the effect of the magnetic field intensity is also appreciable by changing the number of magnets layers. The experimental results show that the magnetic force can be used conveniently as a tuning parameter of the resonance frequency of the suspension, as well as the proof-mass size (Fig. 8).

## 6.2 Applications in the energy harvesting field

One major obstacle the energy harvesting field faces today is lowering the working frequency down to the range of environmental vibrations (1-500 Hz), such as vehicles, machinery, human activities and building oscillations, while keeping the size on a small scale. Most MEMS harvesters have resonance frequencies above 10 kHz, making them difficult to utilize in these applications. The application of a large and heavy proof mass is a strategy used in lowering the resonance frequency in MEMS devices; however they have their own limitations such as a limited withstand weight, small dynamic range, and fatigue in addition to dimension increase. Capacitive electret generators suspended via magnetic levitation can provide an effective design solution to overcome these problems. Electret generators are variable capacitors with a permanent polarized dielectric layer applied to one of the electrode armatures, which can generate electric power output in the presence of vibrations. In the proposed magnetically levitated capacitive generator, the movable electrode corresponds to the graphite proof mass and the fixed electrode is introduced above the graphite proof mass on a rigid support; the electret layer is applied to the upper surface of the proof mass. The schematic representation of a prototype out-of-plane diamagnetically levitated harvester is shown in Fig. 11. The permanent magnets situated in the bottom plane are able to levitate the central mass made with diamagnetic material.

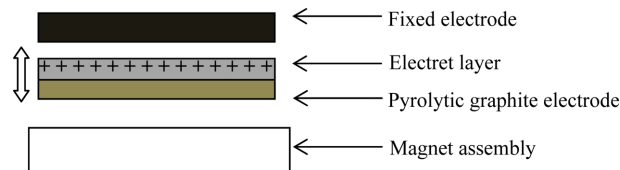


Fig. 11 Magnetically suspended electret capacitive energy harvester based on an out-of-plane kinematic strategy

The harvester introduced by Edamoto (Edamoto *et al.* 2009) is based on electret technology in which a variable capacitor structure is suspended via Parylene high-aspect-ratio spring beams. This harvester was able to generate  $12 \mu W$  at 21 Hz from a  $300 \text{ mm}^2$  area of electrodes. The diamagnetic levitation suspension prototype described in the present study has resonance frequencies ranging from 14 to 19 Hz that provide low stiffness ranging from 2 to 5 N/m for a square shape graphite area varying between  $81$  and  $196 \text{ mm}^2$  respectively (1 mm thickness). Considering the same power per cycle and per unit area of electrode verified by Edamoto, the present harvester is able to generate an output power ranging between  $2.9$  to  $6.3 \mu W$ . The inter-digitized comb drive configuration can be introduced to the perimeter of both electrodes to increase the overlapping active area of the device in order to further increase power output.

## 7. Conclusions

A prototype of the levitating system based on pyrolytic graphite and permanent magnets in the opposite pole configuration was fabricated and employed to investigate the behavior of diamagnetic suspensions. Magnetically levitated system provides lower resonance frequencies and stiffness compare to the mechanically attached counterpart. This represents a promising solution for several applications in both micro and meso scales, such as resonators, RF devices, energy harvesters, inertial sensors, biomedical devices and manipulators. The experimental characterization demonstrates the influence of geometrical parameters on static levitation height, magnetic stiffness, and resonance frequency. The possibility of fine tune the resonance frequency and dynamic response of a system using magnetic force was identified. The application of the diamagnetically levitated suspension to an energy harvester based on the capacitive electret technology has introduced; the estimation of the output power of the generator is provided with reference to the benefits given by the low stiffness suspension. The results obtained from experiments can be modeled with simple relations in the case of small linear oscillations and is useful to optimize the suspension geometry as well as to design a micro-scaled suspension with similar topologies.

## References

- Alqadi, M.K., Al-Khateeb, H.M., Alzoubi, F.Y. and Ayoub, N.Y. (2007), "Effects of magnet size and geometry on magnetic levitation force", *Chinese. Phys. Lett.*, **24**(9), 2664.
- Barrot, F. (2008), *Acceleration and inclination sensors based on magnetic levitation. Application in the particular case of structural health monitoring in civil engineering*, PhD thesis, EPFL, Lausanne, Switzerland.
- Chetouani, H., Delinchant, B. and Reyne, G. (2007), "Efficient modeling approach for optimization of a system based on passive diamagnetic levitation as a platform for bio-medical applications", *Comput. Math. Electric. Eng.*, **26**(2), 345-355.
- Chetouani, H., Haguët, V., Jeandey, C., Pigot, C., Walther, A., Dempsey, N.M., Chatelain, F., Delinchant, B. and Reyne, G. (2007), "Diamagnetic levitation of beads and cells above permanent magnets", *Proceedings of the Transducers and Eurosensors*, Lyon, France, 715-718.
- Chyuan, S.W. and Liao, Y.S. (2005), "Computational study of the effect of finger width and aspect ratios for the electrostatic levitating force of MEMS comb drive", *J. Microelectromech. S.*, **14**(2), 305-312.
- De Pasquale, G., Siyambalapitiya, C., Iamoni, S. and Somà, A. (2010), "Characterization of low-stiffness suspensions based on diamagnetic levitation for MEMS energy harvesters", *Proceedings of the Power MEMS*, Leuven, Belgium, 77-80.

- De Pasquale, G., Siyambalapitiya, C., Somà, A. and Wang, J. (2009), "Performances improvement of MEMS sensors and energy scavengers by diamagnetic levitation", *Proceedings of the ICEAA*, Torino, Italy, 465-468.
- De Pasquale, G., Iamoni, S. and Somà, A. (2012), "3D numerical modeling and experimental validation of diamagnetic levitated suspensions in the static field", Sub. to *Int. J. Mech. Sci.*
- Edamoto, M., Suzuki, Y., Kasagi, N., Kashiwagi, K., Morizawa, Y., Yokohama, T., Seki, T. and Oba, M. (2009), "Low-resonant frequency micro electret generator for energy harvesting application", *Proceedings of the MEMS*, Sorrento, Italy, 1059-1062.
- Elbukem, C., Khamesee, M.B. and Yavuz, M. (2006), "Eddy current damping for magnetic levitation: downscaling from macro- to micro-levitation", *J. Phys. D: Appl. Phys.*, **39**(18), 3932-3938.
- Garnire, D., Choo, H., Kant, R., Govindjee, S., Séquin, C.H., Muller, R.S. and Demmel, J. (2007), "Diamagnetically levitated MEMS accelerometers", *Proceedings of Transducers and Eurosensors*, Lyon, France, 1203-1206.
- Krishnamoorthy, U., Olsson, R.H., Bogart, G.R., Baker, M.S., Carr, D.W., Swiler, T.P. and Clews, P.J. (2008), "In-plane MEMS-based nano-g accelerometer with sub-wavelength optical resonant sensor", *Sensor. Actuat. A - Phys.*, **145-146**, 283-290.
- Mann, B.P. and Sims, N.D. (2009), "Energy harvesting from the nonlinear oscillations of magnetic levitation", *J. Sound Vib.*, **319**(1-2), 515-530.
- Pelrine, R.E. (1995), *Magnetic field levitation*, US Patent, US5396136.
- Tang, W.C., Lim, M.G. and Howe, R.T. (1992), "Electrostatic comb drive levitation and control method", *J. Microelectromech. S.*, **1**(4), 170-178.
- Wei, M., De Pasquale, G., Wang, J. and Somà, A. (2009), "Capacitively-transduced mechanically-coupled bandpass filter in electroplated nickel for harvesting energy from ambient vibrations", *Proceedings of the Power MEMS*, Washington DC, USA, 213-216.
- Yeatman, E.M. (2007), "Applications of MEMS in power sources and circuits", *J. Micromech. Microeng.*, **17**(7), 184-188.